

BIPOLAR IONS EXTRACTION FROM DIELECTRIC BARRIER DISCHARGE

R. MATHON*, N. JIDENKO, J. P. BORRA

Laboratoire de Physique des Gaz et des Plasmas, Équipe Décharges Électriques et Aérosols
(CNRS – Université Paris XI F-91405), Supelec F-91192, France

*E-mail : remi.mathon@u-psud.fr

ABSTRACT

This study aims to develop a post-Dielectric Barrier Discharge (DBD) neutralizer for aerosol (solid or liquid particles suspended in a gas). Indeed, DBD in air, at atmospheric pressure are known to produce bipolar ions required to this application.

This work focuses on ion production, extraction and losses from DBD based on measured post-discharge ions currents. It is shown that post-DBD ion currents depend on discharge electrical properties defining ion production as well as losses in the discharge and in post-discharge related to an electro-hydrodynamic competition. In a plane-to-plane DBD arrangement with wire electrodes, all the filaments have the same charge and energy within 30%. Due to losses, the post-DBD ion currents of both polarities are not proportional to the charge production, related to the time integrated charge per filament. At last, post-DBD ions densities reach the same order of magnitude than those in radioactive neutralizers proving the potentialities of post-DBD aerosol neutralization.

1. INTRODUCTION

The measurement of the size distribution of aerosol is critical for aerosol science and technology. The measuring instrument most commonly used is the Scanning Mobility Particle Sizer (SMPS). The SMPS requires to neutralize aerosol (confer a known charge distribution to solid or liquid particle, centered on zero and depending only on the size of the aerosol). Most of the neutralizers are based on the mechanism of diffusion charging (collisions between ion and particle driven by random ion motion). For this application, ions are commonly produced by radioactive sources such as ^{241}Am , ^{85}Kr and ^{210}Po .

The aerosol charging conditions are defined by the $n_{\text{ion}}\tau$ product (n_{ion} is the ions density and τ the residence time of aerosol in this density). The ions density in a ^{85}Kr charger is about 10^{13} m^{-3} and $n_{\text{ions}}\tau$ product varies from 1.2×10^{13} to $20 \times 10^{13} \text{ s.m}^{-3}$ for flow rates between 5×10^{-6} and $3.3 \times 10^{-5} \text{ m}^{-3}.\text{s}^{-1}$ [1]. Dielectric Barrier Discharge (DBD) produces bipolar ions and is thus an alternative to replace radioactive source commonly used [2][3][4].

In air at atmospheric pressure, the discharge between two planar electrodes occurs as an arc. In DBD, one or several dielectric layer included between the electrodes prevents from arcing. The dielectric layer imposes to operate with alternative voltage with a frequency which depends on the application [5] (for instance ozonizer operates at moderate frequencies -few kHz- to prevent from O_3 destruction for temperature above 100°C).

In air at atmospheric pressure, DBD mainly occurs as numerous filaments homogeneously distributed in time and space. These so-called 'micro-discharges' with diameters of $10\text{-}100 \mu\text{m}$ last a few tens of nanoseconds [5]. One problem of aerosol charging in DBD is the instabilities of the ions source due to aerosol collection on dielectric surfaces. To avoid this, we have chosen to neutralize the aerosol in post-discharge. In a preliminary study at 60 kHz , the maximal ions densities are reached at high voltage ($U_p=10.5 \text{ kV}$) with maximal gas velocity in laminar flow regime [6]. Post-DBD ions densities up to $3.3 \times 10^{13} \text{ m}^{-3}$ for positive ions and $2.4 \times 10^{13} \text{ m}^{-3}$ for negative ions are reached, leading to $n_{\text{ion}}\cdot\tau$ products over $10^{12} \text{ m}^{-3}.\text{s}$, sufficient for aerosol neutralization in post-discharge [6].

This paper aims to depict the influence of thermal and electrical processes on post-discharge ion current. First, electrical characterization of the discharge is described in terms of filaments electrical properties and total charge per period. Finally, the post

discharge ion current and the extraction efficiencies are discussed versus applied voltage.

2. EXPERIMENTAL SET-UP

The experimental set-up is shown on figure 1. A dried and filtered air flow rate of $6.7 \times 10^{-5} \text{ m}^3 \cdot \text{s}^{-1}$ is injected into the DBD.

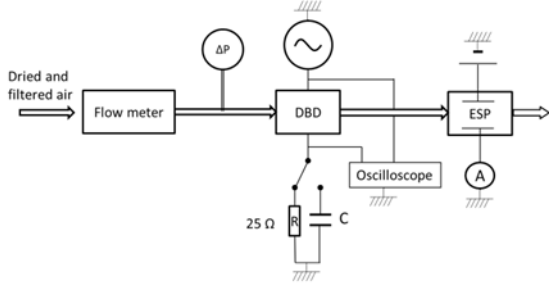


Fig. 1 Experimental set up

The DBD is a plane-to-plane arrangement. Two planes of alumina (thickness of 0.5 mm) are separated by a gap of 0.95 mm. The electrodes are two cylinders of 4 mm diameter and 30 mm length. The flow area is 0.95 mm height \times 36 mm length.

The electrical measurement of DBD is performed with an oscilloscope. A high voltage probe measures the applied voltage (peak voltage, U_p : from 0 to 10 kV and frequency of 63 kHz \pm 1%).

From Lissajou figure, $q(t)=f(u(t))$, using a capacitance of 1 nF, the following parameters are evaluated [7]:

- the energy per period and thus the power consumed by DBD (product of energy per period times the frequency of the applied voltage),

- the capacitances of the dielectric ($C_{dielectrics}$),
- the capacitances of DBD without filaments (C_{DBD}^{off})

- and the total transferred charge per period ($q_{\text{per period}}^{ext}$).

The transferred charge per filaments is measured using a 25 Ω resistor. The measured instantaneous current (i_{mes}) is composed of the capacitive current (i_{capa}) and the current induced in the external circuit by the charge displacement in the gap (i.e. the instantaneous discharge current $i_d^{ext}=i_{mes}-i_{capa}$). So, to measure the transferred charge per filament, the capacitive current has to be suppressed. The transferred charge per filament (q^{ext}) measured in the external circuit is calculated by integration of i_d^{ext} for the filament duration.

The transferred charges, total per period ($q_{\text{per period}}^{ext}$) or per filament (q^{ext}) and the voltage (u_{mes}^{ext}) measured in the external circuit are corrected to evaluate the charge per filament (q^{gas}) and the voltage (v^{gas}) in the gas [8]. The corrected factor ($\alpha_{gas/ext}$) can be written:

$$\alpha_{gas/ext} = \frac{C_{dielectrics}}{C_{dielectrics} - C_{DBD}^{off}}$$

It gives:

$$q^{gas} = \alpha_{gas/ext} \times q^{ext}; \quad v^{gas} = \frac{u_{mes}^{ext}}{\alpha_{gas/ext}}$$

To simplify the notation, all the results are presented with corrected values (i.e. in the gas) but the exponent “gas” will be omitted.

Let us assumed that the input electrical energy is injected only in the discharge filament (i.e. neglecting electrical losses in the external circuit ($< 10\%$), as well as in the dielectric material due to charge displacements in dielectric barriers at high frequencies). So, the energy per filament can be determined directly in the outer circuit from charge measurement using a conversion parameter (U_{conv} , homogeneous to a voltage). This conversion parameter is obtained by the ratio between energy per period and total transferred charge per period in the outer circuit.

To evaluate the post-DBD ion densities, the ion current is measured with an electrometer connected to the collection electrode in a polarized electrostatic precipitator (ESP). Positive and negative currents are measured one after the other.

3. EXPERIMENTAL RESULTS

The post-discharge ions density results from the coupling of the production by filaments, the extraction from the gap and the losses in post discharge. The first step of this study is to control the ion production. The production of ion depends on the charge per filament and the number of filament per period defining the transferred charge per period.

Ion losses are due to recombination, diffusion and electrostatic precipitation induced by electrical forces. The total electric field is the sum of three electric fields: Laplace, space charge and surface charge. The measured current is related to the ratio of ion transit time

(from production to measure) on drift time to the wall. At first approximation, the transit time is controlled by the flow velocity and the dimension of the post discharge.

3.1. Plasma characterization

The aim is to control the plasma in terms of individual filament characteristics and to estimate the transferred charge per period.

3.1.1. Filament characterization

The local ions source is the filament. In a given planar DBD, the filaments present similar transferred charge and energy. Therefore a macroscopic analyze is representative of the local processes around one filament.

To calculate the charge and the energy, the correcting factor and the conversion voltage are evaluated as defined in §2. The correcting factor is $\alpha_{\text{gas/ext}}=1.55 \pm 0.10$. The conversion voltage is $U_{\text{conv}}=4.53$ kV, which represents a voltage of 2.92 kV in the gap. This voltage corresponds to an electric field close to the one required to develop a streamer. It has to be noticed that the conversion voltage depends on the p-d product (with p the pressure and d the gap length) and the temperature of the gas. In our conditions, it can be assumed to be constant.

For an applied voltage of 7.8 kV ($V_p=5$ kV) and a flow rate of $6.7 \times 10^{-5} \text{ m}^3 \cdot \text{s}^{-1}$, the charge distribution of filament is unimodal with a mean of 0.23 nC and is nearly independent of the applied voltage. Close to ambient temperature, the mean energy per filaments is 0.68 μJ .

3.1.2. DBD macroscopic characterization

The total transferred charge in the gap ($q_{\text{per period}}$) is plotted versus the voltage in the gap ($V_p = \frac{U_p}{\alpha_{\text{gas/ext}}}$) with a flow rate of $6.7 \times 10^{-5} \text{ m}^3 \cdot \text{s}^{-1}$ on figure 2.

The $q_{\text{per period}}$ increases nearly linearly with the voltage. As the mean charge per filament is constant (cf. §3.1.1.), the number of filaments also increases linearly with the applied voltage.

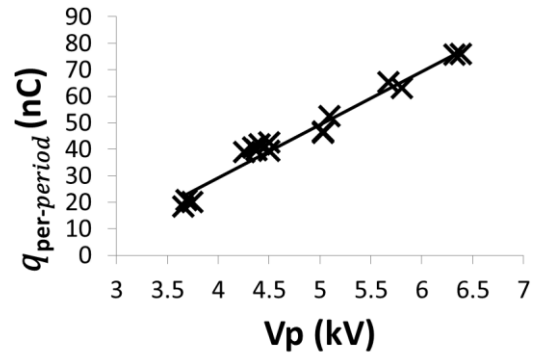


Fig. 2 Transferred charge during one period in function of Vp

To evaluate the charge production term, an equivalent discharge current is defined as the product of the transferred charge per period by the frequency, (e.g. 50 nC per period corresponds to $I_d=3.2$ mA).

For temperature below $\sim 120^\circ\text{C}$, the input power is also linear with the voltage (not presented). $T_{\text{electrode}}$ varies linearly from 35 to 111 $^\circ\text{C}$ with the input power from 3.5 to 13.5 W at $6.7 \times 10^{-5} \text{ m}^3 \cdot \text{s}^{-1}$.

To conclude, the positive and the negative ion productions (assumed to be proportional to discharge current) rise linearly with increasing voltage i.e. with the number of filaments.

3.2. Post-discharge ions current

For a given voltage, in laminar flow regime, ion currents increase with flow rates proving the effect of hydrodynamic condition. Here, positive (I_+), negative (I_-) ions current and extraction efficiencies (I_+/I_d and I_-/I_d) are plotted versus the voltage in the gap for a flow rate of $6.7 \times 10^{-5} \text{ m}^3 \cdot \text{s}^{-1}$.

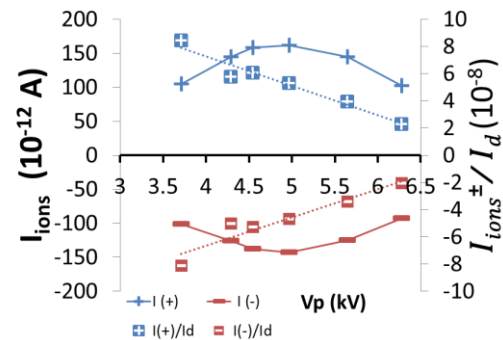


Fig. 3 Ions current and extraction efficiencies versus Vp

Both positive and negative ion currents present a maximum at $V_p=5$ kV. The extraction efficiencies linearly decrease with increasing applied voltage. With increasing voltage, both the production of ions and the ion losses rise. Below 5 kV, the rise of ion production is higher than the losses rise; whereas it is the reverse above 5 kV.

With increasing voltage, Laplace electric field in the gap as well as ion density and related space charge electric field rise. The consequence is an increase of electrical losses and ion recombination. Nevertheless, these effects cannot explain the observed trends. The influence of temperature has to be taken into account. In fact, in similar conditions at lower temperature (with a smaller electrode length of 10 mm instead of 30 mm) the post-discharge ion currents increase on the whole voltage range. This tends to prove that the gas temperature is involved in the presence of a maximum post discharge ion current for the DBD with 3 cm electrode. The temperature affects the mobility and nature of ions, ion diffusion and dielectric surfaces conductivity. The consequence may be an increase of electrical losses at higher temperature. So, ion transport between production and measure is controlled by electro-hydrodynamics equilibrium with temperature affecting both electrical and hydrodynamics processes.

In terms of application, the maximum ion densities are $1.5 \cdot 10^{13} \text{ m}^{-3}$ for positive ions and $1.3 \cdot 10^{13} \text{ m}^{-3}$ for negative ions. These densities are in the same order of magnitude than those in radioactive neutralizers.

CONCLUSION

This experimental study of electrical properties of DBD show that filaments present the same transferred charge and energy within 30%, whatever the voltage is, in a plane-to-plane DBD arrangement using cylinder electrodes.

Post-discharge ion currents are not proportional to ion production due to ions losses. The most probable hypothesis is based on the effect of gas temperature on ions properties (nature and electrical mobility) and related ion losses. Thus, ion transport between production and measure is controlled by electro-hydrodynamics equilibrium with

temperature affecting both electrical and hydrodynamics processes

At last, we have shown that post-DBD ions densities are the same order of magnitude than in radioactive neutralizers. Hence, DBD as bipolar ion source can be used for post-discharge aerosol neutralization. However, O_3 and nanoparticles production has to be controlled for the development of a neutralizer based on DBD.

REFERENCES

- [1] L. B. Modesto-Lopez, E. M. Kettleison and P. Biswas, "Soft X-ray charger (SXC) system for use with electrospray for mobility measurement of bioaerosols", *Journal of electrostatics*, **vol. 69**, no. 4, pp. 357-364, 2011.
- [2] S. B. Kwon, T. Fujimoto, Y. Kuga, H. Sakurai and T. Seto, "Characteristics of aerosol charge distribution by Surface-discharge Microplasma Aerosol Charger (SMAC)", *Aerosol science and Technology*, **vol. 39**, pp. 987-1001, 2005.
- [3] S. Kwon, H. Sakurai, T. Seto and Y. Kim, "Charge neutralization of submicron aerosol using surface-discharge microplasma", *Journal of aerosol science*, **vol. 37**, pp. 483-499, 2005.
- [4] M. Wild, J. Meyer and G. Kasper, "Evaluation of a Drained DBD Electrode Apparatus for Nano-Particle Charging", *EAC, Salzburg*, 2007.
- [5] U. Kogelschatz, B. Eliasson and W. Egli, "Dielectric-barrier discharges : Principle and Applications", *Journal de physique IV*, **vol. 7**, p. C4_47, 1997.
- [6] E. Bourgeois, N. Jidenko, M. Alonso and J. P. Borra, "DBD as a post discharge bipolar ions source and selective ion-induced nucleation versus ion polarity", *Journal of Physics D : Applied Physics*, **vol. 42**, no. 20, p. 205202, 2009.
- [7] A. V. Pipa, T. K. Hoder, J., M. Schmidt and R. Brandenburg, "Experimental determination of dielectric barrier discharge capacitance", *Review of scientific instrument*, **vol. 83**, no. 7, p. 75111, 2012.
- [8] J. Drimal, K. V. Kozlov, V. I. Gibalov and V. G. Samoylovich, "On value of transferred charge in silent discharge under atmospheric pressure", *Czechoslovak Journal of Physics B*, **vol. 38**, no. 2, pp. 159-165, 1988.